

The Skellam Mechanism for Differentially Private Federated Learning

Naman Agarwal* Peter Kairouz† Ziyu Liu‡

Abstract

We introduce the multi-dimensional Skellam mechanism, a discrete differential privacy mechanism based on the difference of two independent Poisson random variables. To quantify its privacy guarantees, we analyze the privacy loss distribution via a numerical evaluation and provide a sharp bound on the Rényi divergence between two shifted Skellam distributions. While useful in both centralized and distributed privacy applications, we investigate how it can be applied in the context of federated learning with secure aggregation under communication constraints. Our theoretical findings and extensive experimental evaluations demonstrate that the Skellam mechanism provides the same privacy-accuracy trade-offs as the continuous Gaussian mechanism, even when the precision is low. More importantly, Skellam is closed under summation and sampling from it only requires sampling from a Poisson distribution – an efficient routine that ships with all machine learning and data analysis software packages. These features, along with its discrete nature and competitive privacy-accuracy trade-offs, make it an attractive practical alternative to the newly introduced discrete Gaussian mechanism.

1 Introduction

The Gaussian mechanism is the workhorse for a multitude of differentially private learning algorithms [46, 10, 1]. While simple enough for mathematical reasoning and privacy accounting analyses, its continuous nature presents a number of challenges in practice. For example, it cannot be exactly represented on finite computers, making it prone to numerical errors that can break its privacy guarantees [35]. Moreover, it cannot be used in distributed learning settings with cryptographic multi-party computation primitives involving modular arithmetic, such as secure aggregation [12, 11]. To address these shortcomings, the binomial and (distributed) discrete Gaussian mechanisms were recently introduced [19, 2, 15, 25]. Unfortunately, both have their own drawbacks: the privacy loss for the binomial mechanism can be infinite with a non-zero probability, and the discrete Gaussian: (a) is not closed under summation (i.e. sum of discrete Gaussians is not a discrete Gaussian), complicating analysis in distributed settings and leading to a performance worse than continuous Gaussian in the highly distributed, low-noise regime [25]; (b) requires a sampling algorithm that is not shipped with mainstream machine learning or data analysis software packages, making it difficult for engineers to use it in production settings (naïve implementations may lead to catastrophic privacy errors).

Our contributions To overcome these limitations, we introduce and analyze the multi-dimensional Skellam mechanism, a mechanism based on adding noise distributed according to the difference of two independent Poisson random variables. The Skellam noise is closed under summation (i.e. sums of Skellam random variables is again Skellam distributed) and can be sampled from easily – efficient Poisson samplers are widely available in numerical software packages. Being discrete in nature also means that it can mesh well cryptographic protocols and can lead to communication savings.

To analyze the privacy guarantees of the Skellam mechanism and compare it with other mechanisms, we

*Google Research namanagarwal@google.com

†Google Research kairouz@google.com

‡Carnegie Mellon University. Work done while at Google Research. ziyuliu@cs.cmu.edu

Alphabetical authorship. Published at the 35th Conference on Neural Information Processing Systems (NeurIPS 2021).

provide a numerical evaluation of the privacy loss random variable and prove a sharp bound on the Rényi divergence between two shifted Skellam distributions. Our careful analysis shows that for a multi-dimensional query function with ℓ_1 sensitivity Δ_1 and ℓ_2 sensitivity Δ_2 , the Skellam mechanism with variance μ achieves $(\alpha, \varepsilon(\alpha))$ Rényi differential privacy (RDP) [36] for $\varepsilon(\alpha) \leq \frac{\alpha \Delta_2}{2\mu} + \min\left(\frac{(2\alpha-1)\Delta_2+6\Delta_1}{4\mu^2}, \frac{3\Delta_1}{2\mu}\right)$ (see Theorem 3.5). This implies that the RDP guarantees are at most $1 + O(1/\mu)$ times worse than those of the Gaussian mechanism.

To analyze the performance of the Skellam mechanism in practice, we consider a differentially private and communication constrained federated learning (FL) setting [26] where the noise is added locally to the d -dimensional discretized client updates that are then summed securely via a cryptographic protocol, such as secure aggregation (SecAgg) [11, 12]. We provide an end-to-end algorithm that appropriately discretizes the data and applies the Skellam mechanism along with modular arithmetic to bound the range of the data and communication costs before applying SecAgg.

We show on distributed mean estimation and two benchmark FL datasets, Federated EMNIST [14] and Stack Overflow [8], that our method can match the performance of the continuous Gaussian baseline under tight privacy and communication budgets, despite using generic RDP amplification via sampling [51] for our approach and the precise RDP analysis for the subsampled Gaussian mechanism [37]. Our method is implemented in TensorFlow Privacy [32] and TensorFlow Federated [24] and will be open-sourced.¹ While we mostly focus on FL applications, the Skellam mechanism can also be applied in other contexts of learning and analytics, including centralized settings.

Related work The Skellam mechanism was first introduced in the context of computational differential privacy from lattice-based cryptography [49] and private Bayesian inference [45]. However, the privacy analyses in the prior work do not readily extend to the multi-dimensional case, and they give direct bounds for pure or approximate DP which makes only advanced composition theorems [28, 22] directly applicable in learning settings where the mechanism is applied many times. For example, the guarantees from [49] lead to poor accuracy-privacy trade-offs as demonstrated in Fig. 1. Moreover, we show in Section 3.1 that extending the direct privacy analysis to the multi-dimensional setting is non-trivial because the worst-case neighboring dataset pair is unknown in this case. For these reasons, our tight privacy analysis via a sharp RDP bound makes the Skellam mechanism practical for learning applications for the first time. These guarantees (almost) match those of the Gaussian mechanism and allow us to use generic RDP amplification via subsampling methods [51].

The closest mechanisms to Skellam are the binomial [2, 19] and the discrete Gaussian mechanisms [15, 25]. The binomial mechanism can (asymptotically) match the continuous Gaussian mechanism (when properly scaled). However, it does not achieve Rényi or zero-concentrated DP [36, 13] and has a privacy loss that can be infinite with a non-zero probability, leading to catastrophic privacy failures. The discrete Gaussian mechanism yields Rényi DP and can be applied to distributed settings [25], but it requires a sampling algorithm that is not yet available in data analysis software packages despite being explored in the lattice-based cryptography community (e.g., [43, 18, 38]). The discrete Gaussian is also not closed under summation and the divergence can be large in highly distributed low-noise settings (e.g. quantile estimation [6] and federated analytics [42]), which causes privacy degradation. See the end of Section 4 for more discussion.

2 Preliminaries

We begin by providing a formal definition for (ε, δ) -differential privacy (DP) [20].

Definition 2.1 (Differential Privacy). *For $\varepsilon, \delta \geq 0$, a randomized mechanism M satisfies (ε, δ) -DP if for all neighboring datasets D, D' and all \mathcal{S} in the range of M , we have that*

$$P(M(D) \in \mathcal{S}) \leq e^\varepsilon P(M(D') \in \mathcal{S}) + \delta,$$

where D and D' are neighboring pairs if they can be obtained from each other by adding or removing all the

¹https://github.com/google-research/federated/tree/master/distributed_dp

records that belong to a particular user.

In our experiments we consider *user-level differential privacy* – i.e., D and D' are neighboring pairs if one of them can be obtained from the other by adding or removing *all* the records associated with a single user [33]. This is stronger than the commonly-used notion of item level privacy where, if a user contributes multiple records, only the addition or removal of one record is protected.

We also make use of Rényi differential privacy (RDP) [36] which allows for tight privacy accounting.

Definition 2.2 (Rényi Differential Privacy). *A mechanism M satisfies (α, ε) -RDP if for any two neighboring datasets D, D' , we have that $D_\alpha(M(D), M(D')) \leq \varepsilon$ where $D_\alpha(P, Q)$ is the Rényi divergence between P and Q and is given by*

$$D_\alpha(P, Q) \triangleq \frac{1}{\alpha - 1} \log \left(\mathbb{E}_{x \sim Q} \left[\left(\frac{P(x)}{Q(x)} \right)^\alpha \right] \right) = \frac{1}{\alpha - 1} \log \left(\mathbb{E}_{x \sim P} \left[\left(\frac{P(x)}{Q(x)} \right)^{\alpha-1} \right] \right).$$

A closely related privacy notion is zero-concentrated DP (zCDP) [21, 13]. In fact, $\frac{1}{2}\varepsilon^2$ -zCDP is equivalent to simultaneously satisfying an infinite family of RDP guarantees, namely $(\alpha, \frac{1}{2}\varepsilon^2\alpha)$ -Rényi differential privacy for all $\alpha \in (1, \infty)$. The following conversion lemma from [13, 15, 7] relates RDP to (ε, δ) -DP.

Lemma 2.3. *If M satisfies (α, ε) -RDP, then, for any $\delta > 0$, M satisfies $(\varepsilon_{DP}(\delta), \delta)$ -DP, where*

$$\varepsilon_{DP}(\delta) = \inf_{\alpha > 1} \varepsilon + \frac{\log(1/\alpha\delta)}{\alpha - 1} + \log(1 - 1/\alpha).$$

For any query function f , we define the Δ_p sensitivity as $\max_{D, D'} \|f(D) - f(D')\|_p$, where D and D' are neighboring pairs differing by adding or removing all the records from a particular user. We also include the RDP guarantees of the discrete Gaussian mechanism (same RDP guarantees as the continuous Gaussian mechanism) to which we compare our method.

Definition 2.4 (The Discrete Gaussian Mechanism [15]). *Given an integer-valued query $f(D) \in \mathbb{Z}^d$ and noise variance μ , the Discrete Gaussian (DGaussian) Mechanism is given by*

$$f(D) + Z, \text{ where } Z \sim \mathcal{N}_{\mathbb{Z}}(0, \mu),$$

and $\mathcal{N}_{\mathbb{Z}}(0, \mu)$ denotes the discrete Gaussian distribution defined in Equation (1) of [15]. The discrete Gaussian mechanism achieves $(\alpha, \frac{\alpha\Delta_2^2}{2\mu})$ -Rényi DP.

3 The Skellam Mechanism

We begin by presenting the definition of the Skellam distribution, which is the basis of the Skellam Mechanism for releasing integer ranged multi-dimensional queries.

Definition 3.1 (Skellam Distribution). *The multidimensional Skellam distribution $\text{Sk}_{\Delta, \mu}$ over \mathbb{Z}^d with mean $\Delta \in \mathbb{Z}^d$ and variance μ is given with each coordinate X_i distributed independently as*

$$X_i \sim \text{Sk}_{\Delta_i, \mu} \text{ with } P(X_i = k) = e^{-\mu} I_{k-\Delta_i}(\mu),$$

for $k \in \mathbb{Z}$. Here, $I_\nu(x)$ is the modified Bessel function of the first kind. A key property of Skellam random variables which motivates their use in DP is that they are closed under summation, i.e. let $X_1 \sim \text{Sk}_{\Delta_1, \mu_1}$ and $X_2 \sim \text{Sk}_{\Delta_2, \mu_2}$ then $X_1 + X_2 \sim \text{Sk}_{\Delta_1 + \Delta_2, \mu_1 + \mu_2}$. This follows from the fact that a Skellam random variable X can be obtained by taking the difference between two independent Poisson random variables with means μ .² We are now ready to introduce the Skellam Mechanism.

²We only consider the symmetric version of Skellam, but it is often more generally defined as the difference of independent Poisson random variables with different variances.

Definition 3.2 (The Skellam Mechanism). *Given an integer-valued query $f(D) \in \mathbb{Z}^d$, we define the Skellam Mechanism as*

$$\text{Sk}_{0,\mu}(f(D)) = f(D) + Z, \text{ where } Z \sim \text{Sk}_{0,\mu},$$

and the total ℓ_2 error of the mechanism is bounded by $\mathbb{E} [\|\text{Sk}_{0,\mu}(f(D)) - f(D)\|_2^2] \leq d\mu$.

The Skellam mechanism was first introduced in [49] for the scalar case. As our goal is to apply the Skellam mechanism in the learning context, we have to address the following challenges. (1) *Tight privacy compositions*: Learning algorithms are iterative in nature and require the application of the DP mechanism many times (often > 1000). The current direct approximate DP analysis in [49] can be combined with advanced composition (AC) theorems [28, 22] but that leads to poor privacy-accuracy trade-offs (see Fig. 1). (2) *Privacy analysis for multi-dimensional queries*: In learning algorithms, the differentially private queries are multi-dimensional (where the dimension equals the number of model parameters, typically $\geq 10^6$). Using composition theorems lead to poor accuracy-privacy trade-offs and a direct extension of approximate DP guarantee [49] for the multi-dimensional case leads to a strong dependence on ℓ_1 sensitivity which is prohibitively large in high dimensions. (3) *Data discretization*: The gradients are naturally continuous vectors but we would like to apply an integer based mechanism. This requires properly discretizing the data while making sure that the norm of the vectors (sensitivity of the query) is preserved. We will tackle challenges (1) and (2) in the remainder of this section and leave (3) for the next section.

3.1 Tight Numerical Accounting via Privacy Loss Distributions

We begin by defining the notion of privacy loss distributions (PLDs).

Definition 3.3 (Privacy Loss Distribution). *For a multi-dimensional discrete privacy mechanism M and neighboring datasets D, D' , for any $x \in \mathbb{Z}^d$, we define $f(x) = \log \left(\frac{P(M(D)=x)}{P(M(D')=x)} \right)$. The privacy loss random variable of M at (D, D') is $Z_{D,D'} = f(M(D))$ [22]. The privacy loss distribution (PLD) of M , denoted by $\text{PLD}_{D,D'}$, is the distribution of $Z_{D,D'}$.*

The PLD of a mechanism M can be used to characterize its (ϵ, δ) -DP guarantees.

Lemma 3.4. *A mechanism M is (ϵ, δ) -DP if and only if $\delta \geq \mathbb{E}_{Z \sim \text{PLD}_{D,D'}} [1 - e^{\epsilon - Z}]_+$ for all neighboring datasets D, D' where $[x]_+ = \max(0, x)$.*

When a mechanism M is applied T times on a dataset, the overall PLD of the composed mechanism at (D, D') is the T -fold convolution of $\text{PLD}_{D,D'}$ [22]. Since discrete convolutions can be computed efficiently using fast Fourier transforms (FFTs) and the expectation in Lemma 3.4 can be numerically approximated, PLDs are attractive for tight numerical accounting [30, 34, 17]. Applying the above to the Skellam mechanism, a direct calculation shows that with X_i are i.i.d. according to $\text{Sk}_{0,\mu}$,

$$Z_{D,D'} = \sum_{i=1}^d \log \left(\frac{I_{X_i - f(D)_i}(\mu)}{I_{X_i - f(D')_i}(\mu)} \right).$$

When $d = 1$, it suffices to look at $Z = \log(I_{X-\Delta}(\mu)/I_X(\mu))$, where $\Delta = \max_{D,D'} |f(D) - f(D')|$ and $X \sim \text{Sk}_{0,\mu}$. Since X has a discrete and symmetric probability distribution and the log function is monotonic, the distribution of Z can be easily characterized. This gives us a tight numerical accountant for the Skellam

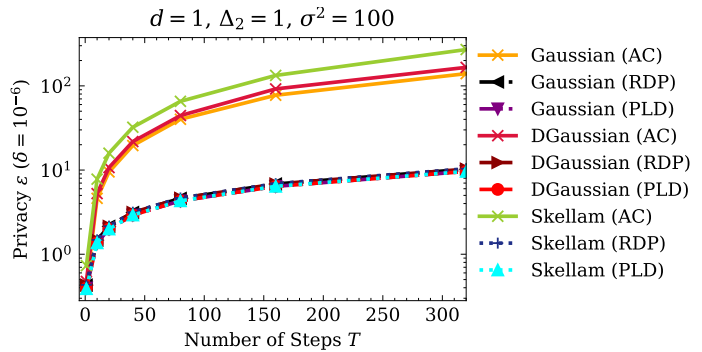


Figure 1: Comparing privacy compositions across various mechanisms and accounting methods.

mechanism in the scalar case, which we use to compare it with both the Gaussian and discrete Gaussian mechanisms. Fig. 1 shows this comparison, highlighting the competitiveness of the Skellam mechanism and the problem of combining the direct analysis of [49] with advanced composition (AC) theorems. When $d > 1$, there are combinatorially many $Z_{D,D'}$'s that need to be considered, even when the ℓ_2 sensitivity of $f(D)$ is bounded. The discrete Gaussian mechanism faces a similar issue (see Theorem 15 of [15]). To provide a tight privacy analysis in the multi-dimensional case, we prove a bound on the RDP guarantees of the Skellam mechanism in the next subsection. Fig. 1 and 2 show that our bound is tight and the competitiveness of the Skellam mechanism in high dimensions.

3.2 Tight Accounting via Rényi Differential Privacy

The following theorem states our main theoretical result, providing a relatively sharp bound on the RDP properties for the Skellam mechanism.

Theorem 3.5. *For $\alpha \in \mathbb{Z}$, $\alpha > 1$ and sensitivity $\Delta \in \mathbb{Z}$, the Skellam Mechanism is (α, ε) -RDP with*

$$\varepsilon(\alpha) \leq \frac{\alpha\Delta^2}{2\mu} + \min\left(\frac{(2\alpha-1)\Delta^2 + 6\Delta}{4\mu^2}, \frac{3\Delta}{2\mu}\right), \quad (3.1)$$

To remind the reader in comparison, the Gaussian mechanism is (α, ε) -RDP with $\varepsilon(\alpha) = \frac{\alpha\Delta^2}{2\mu}$. The bound we provide is at most $1 + O(1/\mu)$ worse than the bound for the Gaussian, which is negligible for all practical choices of μ , especially as the privacy requirements increase.³ Next we show a simple corollary which follows via the independent composition of RDP across dimensions.

Corollary 3.6. *The multi-dimensional Skellam Mechanism is (α, ε) -RDP with*

$$\varepsilon(\alpha) \leq \frac{\alpha\Delta_2^2}{2\mu} + \min\left(\frac{(2\alpha-1)\Delta_2^2 + 6\Delta_1}{4\mu^2}, \frac{3\Delta_1}{2\mu}\right). \quad (3.2)$$

where Δ_1 and Δ_2 are the ℓ_1 and ℓ_2 sensitivities respectively.

3.2.1 Proof Overview for Theorem 3.5

In this subsection, we provide the proof of Theorem 3.5 assuming a technical bound on the ratios of Bessel functions presented as Lemma 3.7, which is the core of our analysis and may be of independent interest. We provide a proof overview for Lemma 3.7, deferring the full proof to the appendix.

On a macroscopic level, our proof structure mimics the RDP proof for the Gaussian mechanism [36], and the main object of our interest is to bound the following quantity, defined for any X, Δ, α :

$$\Phi_{X,\alpha,\Delta}(\mu) \triangleq \log\left(\frac{I_{X-\Delta}(\mu)}{I_{X-\alpha\Delta}(\mu)} \left(\frac{I_{X-\Delta}(\mu)}{I_X(\mu)}\right)^{\alpha-1}\right). \quad (3.3)$$

The following lemma states our main bound on this quantity.

Lemma 3.7. *For any $X, \alpha \in \mathbb{N}$, with $\alpha > 1$ and $\Delta \in \mathbb{Z}$, we have that for all $\mu \geq 0$*

$$\Phi_{X,\alpha,\Delta}(\mu) \leq \frac{\alpha(\alpha-1)\Delta^2}{2\mu} + \min\left(\frac{(2\alpha-1)(\alpha-1)\Delta^2}{4\mu^2} + \frac{3(\alpha-1)|\Delta|}{2\mu^2}, \frac{3(\alpha-1)|\Delta|}{2\mu}\right).$$

Note that in contrast if we consider the analogous notion of Φ for the Gaussian mechanism (replacing $I_X(\mu)$ with the Gaussian density $e^{-X^2/2\mu}$), we readily get the bound $\frac{\alpha(\alpha-1)\Delta^2}{2\mu}$, which is the same as our bound up to lower order terms. We now provide the proof of Theorem 3.5.

³The restriction that α needs to be an integer is a technical one owing to known bounds on Bessel functions. In practice as we show, this restriction has a negligible effect.

Proof of Theorem 3.5. By RDP definition (2.2), we need to bound the following for any $\Delta, \alpha \geq 1$,

$$D_\alpha(\text{Sk}_{\Delta,\mu}, \text{Sk}_{0,\mu}) = \frac{1}{\alpha-1} \log \left(\sum_{X=-\infty}^{\infty} e^{-\mu} I_{X-\Delta}(\mu) \left(\frac{I_{X-\Delta}(\mu)}{I_X(\mu)} \right)^{\alpha-1} \right)$$

Now consider the following calculations on the log term:

$$\begin{aligned} \log \left(\sum_{X=-\infty}^{\infty} \frac{I_{X-\Delta}(\mu)}{e^\mu} \left(\frac{I_{X-\Delta}(\mu)}{I_X(\mu)} \right)^{\alpha-1} \right) &= \log \left(\sum_{X=-\infty}^{\infty} \frac{I_{X-\alpha\Delta}(\mu)}{e^\mu} e^{\Phi_{X,\alpha,\Delta}(\mu)} \right) \\ &\leq \log \left(\sum_{X=-\infty}^{\infty} e^{-\mu} I_{X-\alpha\Delta}(\mu) \right) + \max_{X \in \mathbb{Z}} \Phi_{X,\alpha,\Delta}(\mu) \\ &\leq \frac{\alpha(\alpha-1)\Delta^2}{2\mu} + \min \left(\frac{(2\alpha-1)(\alpha-1)\Delta^2}{4\mu^2} + \frac{3(\alpha-1)|\Delta|}{2\mu^2}, \frac{3(\alpha-1)|\Delta|}{2\mu} \right), \end{aligned}$$

where the inequality follows from Lemma 3.7. \square

We now provide an overview for the proof of Lemma 3.7 highlighting the crux of the argument. As a first step we collect some known facts regarding Bessel functions. It is known that for $x \geq 0$ and $\nu \in \mathbb{Z}, \nu \geq 0$, $I_\nu(x)$ is a decreasing function in ν , $I_{-\nu}(x) = I_\nu(x)$ and $\frac{I_{\nu-1}(\mu)}{I_\nu(x)}$ is an increasing function in ν [47]. A succession of works consider bounding the ratio of successive Bessel functions $I_{\nu-1}(x)/I_\nu(x)$, which is a natural quantity to considering the objective in Lemma 3.7. We use the following very tight characterization for this recently proved in [44, Theorem 5].

Lemma 3.8. *For any $\nu \geq 1/2, x \geq 0$ define the following function we have that*

$$\text{arcsinh}(\delta_0(\nu, x)) \leq \log(I_{\nu-1}(x)) - \log(I_\nu(x)) \leq \text{arcsinh}(\delta_2(\nu, x))$$

where $\delta_\alpha(\nu, x)$ is defined as $\delta_\alpha(\nu, x) \triangleq \frac{\nu-1/2}{x} + \frac{\nu+(\alpha-1)/2}{2x\sqrt{(\nu+(\alpha-1)/2)^2+x^2}}$.

Standard bounds such as those appearing in [5, 49] lead to the following conclusion:

$$\text{arcsinh}((\nu-1/2)/x) \leq \log(I_{\nu-1}(x)) - \log(I_\nu(x)) \leq \text{arcsinh}(\nu/x).$$

While the above bound is significantly easier to work with, it leads to an RDP guarantee of Gaussian RDP + $O(\frac{\Delta}{\mu})$. In high dimensions this manifests as $O(\frac{\Delta}{\mu})$ and overall leads to a constant multiplicative factor over the Gaussian. On the other hand we prove a Gaussian RDP + $o_\mu(1)$ bound. Our proof of Lemma 3.7 splits into various cases depending on the signs of the quantities involved. We show the derivation for a single case below and defer the full proof to the appendix.

Proof of Lemma 3.7 in the case $X \geq \alpha\Delta, \Delta \geq 0$. Replacing $Y = X - \alpha\delta$ we get that

$$\begin{aligned} \Phi_{X,\alpha,\Delta}(\mu) &= \log \left(\frac{I_{Y+(\alpha-1)\Delta}(\mu)}{I_Y(\mu)} \left(\frac{I_{Y+(\alpha-1)\Delta}(\mu)}{I_{Y+\alpha\Delta}(\mu)} \right)^{\alpha-1} \right) \\ &= \sum_{j=0}^{\alpha-2} \left(\sum_{i=Y+j\Delta+1}^{Y+j\Delta+\Delta} \left(\log \left(\frac{I_{i-1+(\alpha-1-j)\Delta}(\mu)}{I_{i+(\alpha-1-j)\Delta}(\mu)} \right) - \log \left(\frac{I_{i-1}(\mu)}{I_i(\mu)} \right) \right) \right) \\ &\leq \sum_{j=0}^{\alpha-2} \left(\sum_{i=Y+j\Delta+1}^{Y+j\Delta+\Delta} (\delta_2(i + (\alpha-1-j)\Delta, \mu) - \delta_0(i, \mu)) \right) \\ &\leq \frac{\alpha(\alpha-1)\Delta^2}{2\mu} + \min \left(\frac{\alpha(\alpha-1)\Delta^2 + 2(\alpha-1)\Delta}{4\mu^2}, \frac{(\alpha-1)\Delta}{2\mu} \right), \end{aligned}$$

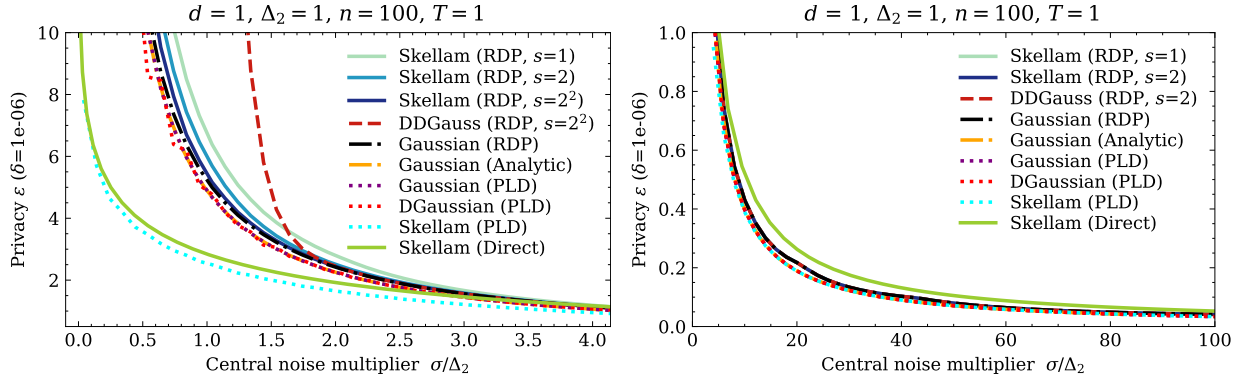


Figure 2: Benchmarking Skellam on sensitivity-1 queries under various accounting methods. RDP: Rényi DP. PLD: privacy loss distributions. Skellam (Direct): [49]. Gaussian (Analytic): [9]. DGaussian [15] / DDGauss [25]: central / distributed discrete Gaussian. s is the scaling factor applied to both Δ and σ . For Skellam and DDGauss [25], the central noise with std σ is split into n shares each applied locally with std σ/\sqrt{n} ; a large n and small σ can thus exacerbate the sum divergence term of DDGauss (left). **Left:** $\varepsilon \leq 10$. **Right:** $\varepsilon \leq 1$.

where the first inequality follows from Lemma 3.8 and the fact that for all $0 \leq x \leq y$, $\operatorname{arcsinh}(y) - \operatorname{arcsinh}(x) \leq y - x$ and the second inequality follows from Lemma A.1 (provided in the appendix):

$$\delta_2(\nu_1, x) - \delta_0(\nu_2, x) \leq \frac{\nu_1 - \nu_2}{x} + \frac{1}{2x} \min\left(\frac{\nu_1 - \nu_2 + 1}{x}, 1\right).$$

□

4 Applying the Skellam Mechanism to Federated Learning

With a sharp RDP analysis for the multi-dimensional Skellam mechanism presented in the previous section, we are now ready to apply it to differentially private federated learning. We first outline the general problem setting and then describe our approach under central and distributed DP models.

Problem setting At a high-level, we consider the distributed mean estimation problem. There are n clients each holding a vector x_i in \mathbb{R}^d such that for all i , the vector norm is bounded as $\|x_i\|_2 \leq c$ for some $c \geq 0$. We denote the set of vectors as $\mathcal{X} = \{x_i\}_{i=1}^n$, and the aim is for each client to communicate the vectors x_i to a central server which then aggregates them as $\hat{x} = \frac{1}{n} \sum_i x_i$ for an external analyst. In federated learning, the client vectors x_i are the model gradients or model deltas (typically $d \geq 10^6$) after training on the clients' local datasets, and this procedure can be repeated for many rounds ($T > 1000$). A large d and T thus necessitate accounting methods that provide tight privacy compositions for high-dimensional queries.

We are primarily concerned with three metrics for this procedure and their trade-offs: (1) *Privacy*: the mean \hat{x} should be differentially private with a reasonably small (ε, δ) ; (2) *Error*: we wish to minimize the expected ℓ_2 error; and (3) *Communication*: we wish to minimize the average number of bits communicated per coordinate. Characterizing this trade-off is an important research problem. For example, it has been recently shown [50] that without formal privacy guarantees, the client training data could still be revealed by the model updates x_i ; on the other hand, applying differential privacy [48] to these updates can degrade the final utility.

Skellam for central DP The central DP model refers to adding Skellam noise onto the non-private aggregate \hat{x} before releasing it to the external analyst. One important consideration is that the model updates in FL are continuous in nature, while Skellam is a discrete probability distribution. One approach is to appropriately discretize the client updates, e.g., via uniform quantization (which involves scaling the inputs by

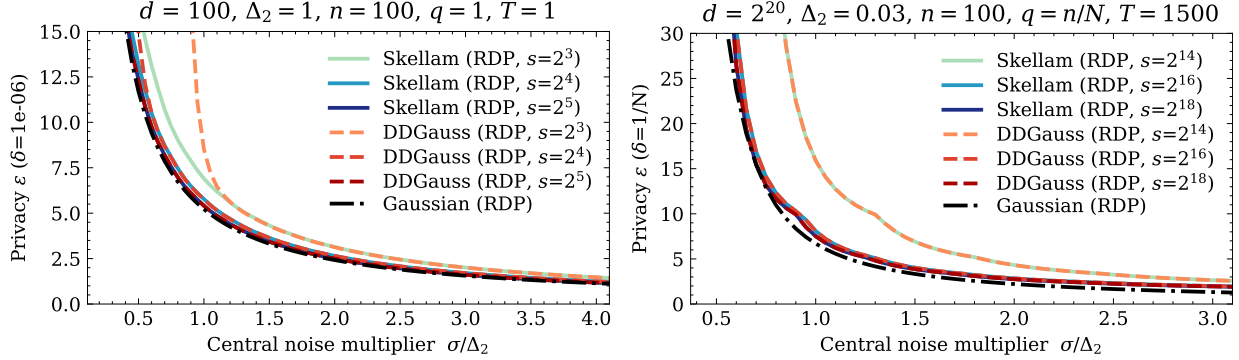


Figure 3: Comparing Skellam and Distributed Discrete Gaussian (DDGauss) on multi-dimensional real-valued queries, rounded to integers with $\beta = e^{-0.5}$ (Prop. 4.2). s is the scaling applied to both σ and Δ_2 ; a larger s reduces the rounding error and norm inflation. q is the sampling rate. For Skellam and DDGauss [25], the central noise with std σ is split into n shares each applied locally with std σ/\sqrt{n} ; a large n and small σ can exacerbate the sum divergence term of DDGauss. **Left:** Simple setting with $\Delta_2 = 1$. **Right:** FL-like setting for training CNNs on Federated EMNIST.

a factor $s \sim 2^b$ for some bit-width b followed by stochastic rounding⁴ for unbiased estimates), and the server can convert the private aggregate back to real numbers at the end. Note that this allows us to re-parameterize the variance of the added Skellam noise as $s^2\mu$, giving the following simple corollary based on Cor. 3.6:

Corollary 4.1 (Scaled Skellam Mechanism). *With a scaling factor $s \in \mathbb{R}$, the multi-dimensional Skellam Mechanism is (α, ε) -RDP with*

$$\varepsilon(\alpha) \leq \frac{\alpha\Delta_2^2}{2\mu} + \min\left(\frac{(2\alpha-1)\Delta_2^2}{4s^2\mu^2} + \frac{3\Delta_1}{2s^3\mu^2}, \frac{3\Delta_1}{2s\mu}\right). \quad (4.1)$$

As s increases, the RDP of scaled Skellam rapidly approaches that of Gaussian as the second term above approaches 0, suggesting that under practical regimes with moderate compression bit-width, Skellam should perform competitively compared to Gaussian. Another aspect worth noting is that rounding vector coordinates from reals to integers can inflate the ℓ_2 -sensitivity Δ_2 , and thus more noise is required for the same privacy. To this end, we leverage the *conditional rounding* procedure introduced in [25] to obtain a bounded norm on the scaled and rounded client vector:

Proposition 4.2 (Norm of stochastically rounded vector [25]). *Let \tilde{x} be a stochastic rounding of vector $x \in \mathbb{R}^d$ to the integer grid \mathbb{Z}^d . Then, for $\beta \in (0, 1)$, we have*

$$\mathbb{P}\left[\|\tilde{x}\|_2^2 \leq \|x\|_2^2 + d/4 + \sqrt{2\log(1/\beta)} \cdot (\|x\|_2 + \sqrt{d}/2)\right] \geq 1 - \beta. \quad (4.2)$$

Conditional rounding is thus defined as retrying the stochastic rounding on x_i until $\|\tilde{x}_i\|_2^2$ is within the probabilistic bound above (which also gives the inflated sensitivity $\tilde{\Delta}_2$). We can then add Skellam noise to the aggregate $\sum_i \tilde{x}_i$ according to $\tilde{\Delta}_2$ before undoing the quantization (unscaling). Note that a larger scaling s before rounding reduces the norm inflation and the extra noise needed (Fig. 3 right).

Skellam for distributed DP with secure aggregation A stronger notion of privacy in FL can be obtained via the distributed DP model [25] that leverages secure aggregation (SecAgg [12]). The fact that the Skellam distribution is closed under summation allows us to easily extend from central DP to distributed DP. Under this model, the client vectors are quantized as in central DP model, but the Skellam noise is now added locally with variance μ/n . Then, the noisy client updates are summed via SecAgg (b bits per

⁴Example of stochastic rounding: 42.3 has 0.7 and 0.3 probability to be rounded to 42 and 43, respectively. Other discretization schemes are possible; we do not explore this direction further in this work.

coordinate for field size 2^b) which only reveals the noisy aggregate to the server. While the local noise might be insufficient for local DP guarantees, the aggregated noise at the server provides privacy and utility comparable to the central DP model, thus removing trust away from the central aggregator. Note that the modulo operations introduced by SecAgg does not impact privacy as it can be viewed as a post-processing of an already differentially private query.

We remark on several properties of the distributed Skellam compared to the distributed discrete Gaussian (DDGauss [25]). (1) DDGauss is not closed under summation, and the divergence between discrete Gaussians can lead to notable privacy degradation in settings such as quantile estimation [6] and federated analytics [42] with sufficiently large number of clients and small local noises (see also the left side of Fig. 2 and Fig. 3). While scaling mitigates this issue, it also requires additional bit-width which makes Skellam attractive under tight communication constraints. (2) Sampling from Skellam only requires sampling from Poisson, for which efficient implementations are widely available in numerical software packages. While efficient discrete Gaussian sampling has also been explored in the lattice-based cryptography community (e.g., [43, 18, 38]), we believe the accessibility of Skellam samplers would help facilitate the deployment of DP to FL settings with mobile and edge devices. See Appendix D for more discussion. (3) In practice where $s \gg 1$ (dictated by bit-width b), both Skellam (cf. Cor. 4.1) and DDGauss (with an exponentially small divergence) quickly approaches Gaussian under RDP, and any differences will be negligible (Fig. 3).

5 Empirical Evaluation

In this section, we empirically evaluate the Skellam mechanism on two sets of experiments: distributed mean estimation and federated learning. In both cases, we focus on the distributed DP model, but note that the Skellam mechanism can be easily adapted to the central DP setting as discussed in the earlier section. Unless otherwise stated, we use RDP accounting for all experiments due to the high-dimensional data and the ease of composition (Section 3). To obtain Δ_1 for Skellam RDP, we note that $\Delta_1 \leq \Delta_2 \cdot \min(\sqrt{d}, \Delta_2)$ since $\Delta_1 \leq \sqrt{d}\Delta_2$ in general and $\Delta_1 \leq \Delta_2^2$ for integers.

Under the distributed DP model, we also introduce a random orthogonal transformation [29, 2, 25] before discretizing and aggregating the client vectors (which can be reverted after the aggregation); this makes the vector coordinates sub-Gaussian and helps spread the magnitudes of the vector coordinates across all dimensions, thus reducing the errors from quantization and potential wrap-around from SecAgg modulo operations. Moreover, by approximating the sub-exponential tail of the Skellam distribution as sub-Gaussian, we can derive a heuristic for choosing s following [25] based on a bound on the variance $\tilde{\sigma}^2$ of the aggregated signal, as $\tilde{\sigma}^2 \leq c^2 n^2/d + n/(4s^2) + \mu$. We choose s such that $2k\tilde{\sigma}$ are bounded within the SecAgg field size 2^b , where k is a small constant.

Algorithm 1 summarizes the aggregation procedure for the distributed Skellam mechanism via secure aggregation as well as the parameters used for the experiments. In summary, we have an ℓ_2 clip norm $c > 0$; per-coordinate bit-width b ; target central noise variance $\mu > 0$; number of clients n ; signal bound multiplier $k > 0$; and rounding bias $\beta \in [0, 1)$. We fix $\beta = e^{-1/2}$ for all experiments. Note that the per-coordinate bit-width b is for the aggregated sum as it determines the field size of SecAgg. For federated learning, we also consider the number of rounds T and the total number of clients N (thus the uniform sampling ratio $q = n/N$ at every round). Our experiments are implemented in Python, TensorFlow Privacy [32], and TensorFlow Federated [24]. See also Appendix for additional results and more details on the experimental setup.

5.1 Distributed Mean Estimation (DME)

We first consider DME as the generalization of (single round) FL. We randomly generate n client vectors $X = \{x_i\}_{i=1}^n$ from the d -dimensional ℓ_2 sphere with radius $c = 10$, and compute the true mean $\hat{x} = \frac{1}{n} \sum_{i=1}^n x_i$. We then compute the private estimate of \hat{x} with the distributed Skellam mechanism (Algorithm 1) as \bar{x} . For a strong baseline, we use the analytic Gaussian mechanism [9] with tight accounting (see also Figure 2). In Figure 4, we plot the MSE as $\|\hat{x} - \bar{x}\|_2^2/d$ with 95% confidence interval (small shaded region) over 10 dataset initializations across different values of b , d , and n . Results demonstrate that Skellam can match Gaussian

Algorithm 1 Aggregation Procedure for the Distributed Skellam Mechanism

Inputs: Private vector $x_i \in \mathbb{R}^{\bar{d}}$ for each client i ; ℓ_2 clip norm $c > 0$; Bit-width b ; Target central noise variance $\mu > 0$; Number of clients n ; Signal bound multiplier $k > 0$; Bias $\beta \in [0, 1)$.

Shared randomness: $d \times d$ diagonal matrix D with uniformly random $\{-1, +1\}$ values, where $d \geq \bar{d}$ is the nearest power of 2.

Shared scale: Obtain scaling factor s such that $2^b = 2k\tilde{\sigma} = 2k\sqrt{c^2n^2/d + n/(4s^2) + \mu}$.

Procedure CLIENTPROCEDURE(x_i, s, D)

Clip and scale vector $\hat{x}_i = s \cdot \min(1, c/\|x_i\|_2) \cdot x_i$, and pad to \bar{d} dimensions with zeros.

Random rotation: $\tilde{x}_i = \tilde{H}_d D \hat{x}_i$ where $\tilde{H}_d = \frac{1}{\sqrt{d}} H_d$ is the normalized $d \times d$ Hadamard matrix.

repeat {conditional stochastic rounding}

 Stochastically round the coordinates of \tilde{x}_i to the integer grid to produce \tilde{x}_i

until $\|\tilde{x}_i\|_2^2 \leq \min \left\{ (sc + \sqrt{d})^2, s^2c^2 + d/4 + \sqrt{2 \log(1/\beta)} \cdot (sc + \sqrt{d}/2) \right\}$.

Local noising: Sample noise vector $y_i \in \mathbb{Z}^d$ where each entry is sampled from $\text{Sk}_{0, s^2\mu/n}$.

return $z_i = \tilde{x}_i + y_i$ under the SecAgg protocol with modulo bit-width b .

Procedure SERVERPROCEDURE(z, s, D) { z is the modular sum of z_i under bit-width b }

return $\bar{x} = \frac{1}{s} D \tilde{H}_d^\top z$, with $\bar{x} \approx \sum_i x_i \in \mathbb{R}^d$.

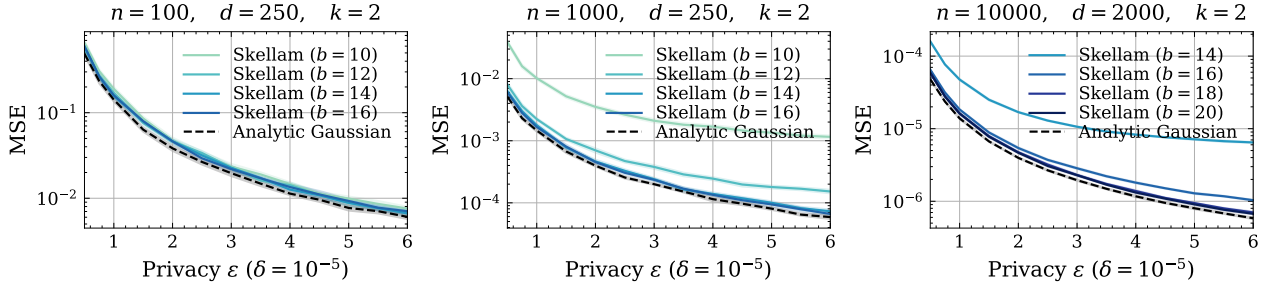


Figure 4: Distributed mean estimation with the distributed Skellam mechanism.

even with $n = 10000$ clients as long as the bit-width is sufficient. We emphasize that the communication cost b depends logarithmically on n , and to put numbers into context, Google’s production next-word prediction models [23, 39] use $n \leq 500$ and the production DP language model [40] uses $n = 20000$.

5.2 Federated Learning

Setup We evaluate on three public federated datasets with real-world characteristics: Federated EMNIST [16], Shakespeare [31, 14], and Stack Overflow next word prediction (SO-NWP [8]). EMNIST is an image classification dataset for hand-written digits and letters; Shakespeare is a text dataset for next-character-prediction based on the works of William Shakespeare; and SO-NWP is a large-scale text dataset for next-word-prediction based on user questions/answers from stackoverflow.com. We emphasize that all datasets have natural client heterogeneity that are representative of practical FL problems: the images in EMNIST are grouped the writer of the handwritten digits, the lines in Shakespeare are grouped by the speaking role, and the sentences in SO-NWP are grouped by the corresponding Stack Overflow user. We train a small CNN with model size $\bar{d} < 2^{20}$ for EMNIST and use the recurrent models defined in [41] for Shakespeare and SO-NWP. The hyperparameters for the experiments follow those from [25, 6, 27, 41] and tuning is limited. For EMNIST, we follow [25] and fix $c = 0.03$, $n = 100$, $T = 1500$, client learning rate $\eta_{\text{client}} = 0.32$, server learning rate $\eta_{\text{server}} = 1$, and client batch size $m = 20$. For Shakespeare, we follow [6] and fix $n = 100$, $T = 1200$, $\eta_{\text{client}} = 1$, $\eta_{\text{server}} = 0.32$, and $m = 4$, and we sweep $c \in \{0.25, 0.5\}$. For SO-NWP, we follow [27] and fix $c = 0.3$, $n = 100$, $T = 1600$, $\eta_{\text{client}} = 0.5$, and $m = 16$, and we sweep $\eta_{\text{server}} \in \{0.3, 1\}$ and limit max examples per client to 256. In all cases, clients train for 1 epoch on their local datasets, and

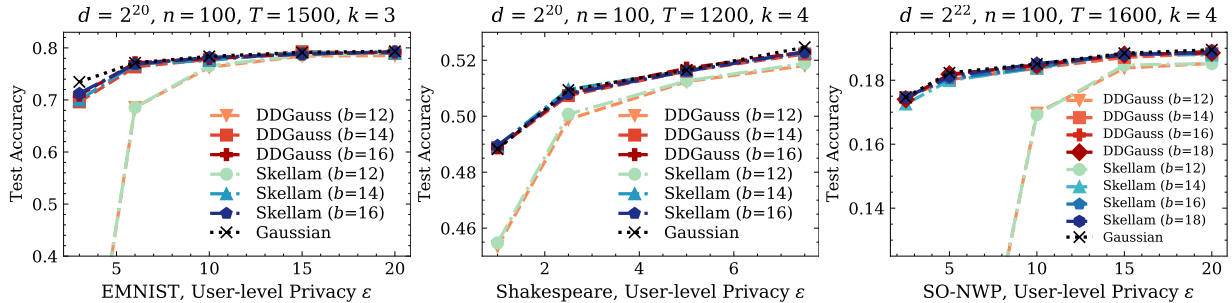


Figure 5: Federated learning with the distributed Skellam mechanism. DDGauss: Distributed Discrete Gaussian [25]. **Left / Middle / Right:** Test accuracies on EMNIST / Shakespeare / Stack Overflow NWP across different ϵ and b . δ is set to $1/N$, 10^{-6} , 10^{-6} , respectively. For Shakespeare, privacy is reported with a hypothetical population size $N = 10^6$.

the client updates are weighted uniformly (as opposed to weighting by number of examples). See Appendix for more results and full details on datasets, models, and hyperparameters.

Results Figure 5 summarizes the FL experiments. For EMNIST and Shakespeare, we report the average test accuracy over the last 100 rounds. For SO-NWP, we report the top-1 accuracy (without padding, out-of-vocab, or beginning/end-of-sentence tokens) on the test set. The results indicate that Skellam performs as good as Gaussian despite relying on generic RDP amplification via sampling [51] (cf. Fig. 3) and that Skellam matches DDG consistently under realistic regimes. This bears significant practical relevance given the advantages of Skellam over DDG in real-world deployments.

6 Conclusion

We have introduced the multi-dimensional Skellam mechanism for federated learning. We analyzed the Skellam mechanism through the lens of approximate DP, privacy loss distributions, and Rényi divergences, and derived a sharp RDP bound that enables Skellam to match Gaussian and discrete Gaussian in practical settings as demonstrated by our large-scale experiments. Since Skellam is closed under summation and efficient samplers are widely available, it represents an attractive alternative to distributed discrete Gaussian as it easily extends from the central DP model to the distributed DP model. Being a discrete mechanism can also bring potential communication savings over continuous mechanisms and make Skellam less prone to attacks that exploit floating-point arithmetic on digital computers. Some interesting future work includes: (1) our scalar PLD analysis for Skellam suggests room for improvements on our multi-dimensional analysis via a complete PLD characterization, and (2) our results on FL may be further improved via a targeted analysis for RDP amplification via sampling akin to [37]. Overall, this work is situated within the active area of private machine learning and aims at making ML more trustworthy. One potential negative impact is that our method could be (deliberately or inadvertently) misused, such as sampling the wrong noise or using a minuscule scaling factor, to provide non-existent privacy guarantees for real users’ data. We nevertheless believe our results have positive impact as they facilitate the deployment of differential privacy in practice.

References

- [1] Martin Abadi, Andy Chu, Ian Goodfellow, H Brendan McMahan, Ilya Mironov, Kunal Talwar, and Li Zhang. Deep learning with differential privacy. In *Proceedings of the 2016 ACM SIGSAC conference on computer and communications security*, pages 308–318, 2016.
- [2] Naman Agarwal, Ananda Theertha Suresh, Felix Xinnan X Yu, Sanjiv Kumar, and Brendan McMahan. cpSGD: Communication-efficient and differentially-private distributed sgd. In *Advances in Neural Information Processing Systems*, pages 7564–7575, 2018.
- [3] Maruan Al-Shedivat, Jennifer Gillenwater, Eric Xing, and Afshin Rostamizadeh. Federated learning via posterior averaging: A new perspective and practical algorithms. In *ICLR*, 2021.
- [4] Martin R. Albrecht and Michael Walter. dgs, Discrete Gaussians over the Integers. Available at <https://bitbucket.org/malb/dgs>, 2018.
- [5] Donald E Amos. Computation of modified bessel functions and their ratios. *Mathematics of Computation*, 28(125):239–251, 1974.
- [6] Galen Andrew, Om Thakkar, H Brendan McMahan, and Swaroop Ramaswamy. Differentially private learning with adaptive clipping. *arXiv preprint arXiv:1905.03871*, 2019.
- [7] S. Asoodeh, J. Liao, F. P. Calmon, O. Kosut, and L. Sankar. A better bound gives a hundred rounds: Enhanced privacy guarantees via f-divergences. In *2020 IEEE International Symposium on Information Theory (ISIT)*, pages 920–925, 2020.
- [8] The TensorFlow Federated Authors. Tensorflow federated stack overflow dataset, 2019.
- [9] Borja Balle and Yu-Xiang Wang. Improving the gaussian mechanism for differential privacy: Analytical calibration and optimal denoising. In *International Conference on Machine Learning*, pages 394–403. PMLR, 2018.
- [10] Raef Bassily, Adam Smith, and Abhradeep Thakurta. Private empirical risk minimization: Efficient algorithms and tight error bounds. In *2014 IEEE 55th Annual Symposium on Foundations of Computer Science*, pages 464–473. IEEE, 2014.
- [11] James Bell, K. A. Bonawitz, Adrià Gascón, Tancrede Lepoint, and Mariana Raykova. Secure single-server aggregation with (poly)logarithmic overhead. Cryptology ePrint Archive, Report 2020/704, 2020. <https://eprint.iacr.org/2020/704>.
- [12] Keith Bonawitz, Vladimir Ivanov, Ben Kreuter, Antonio Marcedone, H Brendan McMahan, Sarvar Patel, Daniel Ramage, Aaron Segal, and Karn Seth. Practical secure aggregation for privacy-preserving machine learning. In *proceedings of the 2017 ACM SIGSAC Conference on Computer and Communications Security*, pages 1175–1191, 2017.
- [13] Mark Bun and Thomas Steinke. Concentrated differential privacy: Simplifications, extensions, and lower bounds. In *Theory of Cryptography Conference*, pages 635–658. Springer, 2016.
- [14] Sebastian Caldas, Sai Meher Karthik Duddu, Peter Wu, Tian Li, Jakub Konečný, H Brendan McMahan, Virginia Smith, and Ameet Talwalkar. Leaf: A benchmark for federated settings. *arXiv preprint arXiv:1812.01097*, 2018.
- [15] Clément Canonne, Gautam Kamath, and Thomas Steinke. The discrete gaussian for differential privacy. In *NeurIPS*, 2020.
- [16] Gregory Cohen, Saeed Afshar, Jonathan Tapson, and Andre Van Schaik. Emnist: Extending mnist to handwritten letters. In *2017 International Joint Conference on Neural Networks (IJCNN)*, pages 2921–2926. IEEE, 2017.
- [17] Google Differential Privacy Team. Privacy loss distributions. https://github.com/google/differential-privacy/blob/master/accounting/docs/Privacy_Loss_Distributions.pdf. 2020.
- [18] Nagarjun C Dwarakanath and Steven D Galbraith. Sampling from discrete gaussians for lattice-based cryptography on a constrained device. *Applicable Algebra in Engineering, Communication and Computing*, 25(3):159–180, 2014.

- [19] Cynthia Dwork, Krishnaram Kenthapadi, Frank McSherry, Ilya Mironov, and Moni Naor. Our data, ourselves: Privacy via distributed noise generation. In *Annual International Conference on the Theory and Applications of Cryptographic Techniques*, pages 486–503. Springer, 2006.
- [20] Cynthia Dwork, Frank McSherry, Kobbi Nissim, and Adam Smith. Calibrating noise to sensitivity in private data analysis. In *Theory of cryptography conference*, pages 265–284. Springer, 2006.
- [21] Cynthia Dwork and Guy N Rothblum. Concentrated differential privacy. *arXiv preprint arXiv:1603.01887*, 2016.
- [22] Cynthia Dwork, Guy N Rothblum, and Salil Vadhan. Boosting and differential privacy. In *2010 IEEE 51st Annual Symposium on Foundations of Computer Science*, pages 51–60. IEEE, 2010.
- [23] Andrew Hard, Kanishka Rao, Rajiv Mathews, Swaroop Ramaswamy, Françoise Beaufays, Sean Augenstein, Hubert Eichner, Chloé Kiddon, and Daniel Ramage. Federated learning for mobile keyboard prediction. *arXiv preprint arXiv:1811.03604*, 2018.
- [24] Alex Ingerman and Krzys Ostrowski. Introducing tensorflow federated, 2019.
- [25] Peter Kairouz, Ziyu Liu, and Thomas Steinke. The distributed discrete gaussian mechanism for federated learning with secure aggregation. In *International Conference on Machine Learning*. PMLR, 2021.
- [26] Peter Kairouz, Brendan McMahan, et al. Advances and open problems in federated learning. *arXiv preprint arXiv:1912.04977*, 2019.
- [27] Peter Kairouz, Brendan McMahan, Shuang Song, Om Thakkar, Abhradeep Thakurta, and Zheng Xu. Practical and private (deep) learning without sampling or shuffling. *arXiv preprint arXiv:2103.00039*, 2021.
- [28] Peter Kairouz, Sewoong Oh, and Pramod Viswanath. The composition theorem for differential privacy. In *International conference on machine learning*, pages 1376–1385. PMLR, 2015.
- [29] Jakub Konečný, H Brendan McMahan, Felix X Yu, Peter Richtárik, Ananda Theertha Suresh, and Dave Bacon. Federated learning: Strategies for improving communication efficiency. *arXiv preprint arXiv:1610.05492*, 2016.
- [30] Antti Koskela, Joonas Jälkö, and Antti Honkela. Computing tight differential privacy guarantees using fft. In *International Conference on Artificial Intelligence and Statistics*, pages 2560–2569. PMLR, 2020.
- [31] Brendan McMahan, Eider Moore, Daniel Ramage, Seth Hampson, and Blaise Aguerre y Arcas. Communication-efficient learning of deep networks from decentralized data. In *Artificial Intelligence and Statistics*, pages 1273–1282, 2017.
- [32] H Brendan McMahan, Galen Andrew, Ulfar Erlingsson, Steve Chien, Ilya Mironov, Nicolas Papernot, and Peter Kairouz. A general approach to adding differential privacy to iterative training procedures. *arXiv preprint arXiv:1812.06210*, 2018.
- [33] H Brendan McMahan, Daniel Ramage, Kunal Talwar, and Li Zhang. Learning differentially private recurrent language models. In *ICLR*, 2018.
- [34] Sebastian Meiser and Esfandiar Mohammadi. Tight on budget? tight bounds for r-fold approximate differential privacy. In *Proceedings of the 2018 ACM SIGSAC Conference on Computer and Communications Security*, pages 247–264, 2018.
- [35] Ilya Mironov. On significance of the least significant bits for differential privacy. In *Proceedings of the 2012 ACM conference on Computer and communications security*, pages 650–661, 2012.
- [36] Ilya Mironov. Rényi differential privacy. In *2017 IEEE 30th Computer Security Foundations Symposium (CSF)*, pages 263–275. IEEE, 2017.
- [37] Ilya Mironov, Kunal Talwar, and Li Zhang. Rényi differential privacy of the sampled gaussian mechanism. *arXiv preprint arXiv:1908.10530*, 2019.
- [38] Thomas Prest, Thomas Ricosset, and Mélissa Rossi. Simple , fast and constant-time gaussian sampling over the integers for falcon. In *Second PQC Standardization Conference*, 2019.

- [39] Swaroop Ramaswamy, Rajiv Mathews, Kanishka Rao, and Françoise Beaufays. Federated learning for emoji prediction in a mobile keyboard. *arXiv preprint arXiv:1906.04329*, 2019.
- [40] Swaroop Ramaswamy, Om Thakkar, Rajiv Mathews, Galen Andrew, H Brendan McMahan, and Françoise Beaufays. Training production language models without memorizing user data. *arXiv preprint arXiv:2009.10031*, 2020.
- [41] Sashank Reddi, Zachary Charles, Manzil Zaheer, Zachary Garrett, Keith Rush, Jakub Konečný, Sanjiv Kumar, and H Brendan McMahan. Adaptive federated optimization. *arXiv preprint arXiv:2003.00295*, 2020.
- [42] Google Research. Federated analytics: Collaborative data science without data collection, May 2020.
- [43] Sujoy Sinha Roy, Frederik Vercauteren, and Ingrid Verbauwhede. High precision discrete gaussian sampling on fpgas. In *International Conference on Selected Areas in Cryptography*, pages 383–401. Springer, 2013.
- [44] Diego Ruiz-Antolín and Javier Segura. A new type of sharp bounds for ratios of modified bessel functions. *Journal of Mathematical Analysis and Applications*, 443(2):1232–1246, 2016.
- [45] Aaron Schein, Zhiwei Steven Wu, Alexandra Schofield, Mingyuan Zhou, and Hanna Wallach. Locally private bayesian inference for count models. In *International Conference on Machine Learning*, pages 5638–5648. PMLR, 2019.
- [46] Shuang Song, Kamalika Chaudhuri, and Anand D Sarwate. Stochastic gradient descent with differentially private updates. In *2013 IEEE Global Conference on Signal and Information Processing*, pages 245–248. IEEE, 2013.
- [47] VR Thiruvenkatachar and TS Nanjundiah. Inequalities concerning bessel functions and orthogonal polynomials. In *Proceedings of the Indian Academy of Sciences-Section A*, volume 33, page 373. Springer, 1951.
- [48] Florian Tramèr and Dan Boneh. Differentially private learning needs better features (or much more data). *arXiv preprint arXiv:2011.11660*, 2020.
- [49] Filipp Valovich and Francesco Alda. Computational differential privacy from lattice-based cryptography. In *International Conference on Number-Theoretic Methods in Cryptology*, pages 121–141. Springer, 2017.
- [50] Hongxu Yin, Arun Mallya, Arash Vahdat, Jose M Alvarez, Jan Kautz, and Pavlo Molchanov. See through gradients: Image batch recovery via gradinversion. *arXiv preprint arXiv:2104.07586*, 2021.
- [51] Yuqing Zhu and Yu-Xiang Wang. Poission subsampled rényi differential privacy. In *International Conference on Machine Learning*, pages 7634–7642. PMLR, 2019.

A Proof of Lemma 3.7

Before moving forward we state the following lemma which follows via a simple calculation.

Lemma A.1. *For any positive real number $\nu \geq 1/2$ and any $x \geq 0$, we have that*

$$\delta_0(\nu, x) \geq \frac{\nu - 1/2}{x}$$

$$\delta_2(\nu, x) \leq \min\left(\frac{\nu - 1/2}{x} \left(1 + \frac{1}{2x}\right) + \frac{1}{2x^2}, \frac{\nu - 1/2}{x} + \frac{1}{2x}\right).$$

Further for any positive reals $\nu_1 \geq \nu_2, x$ we have that

$$\delta_2(\nu_1, x) - \delta_0(\nu_2, x) \leq \frac{\nu_1 - \nu_2}{x} + \frac{1}{2x} \min\left(\frac{\nu_1 - \nu_2 + 1}{x}, 1\right)$$

where $\delta_\alpha(\nu, x) \triangleq \frac{\nu - 1/2}{x} + \frac{\nu + (\alpha - 1)/2}{2x\sqrt{(\nu + (\alpha - 1)/2)^2 + x^2}}$ as defined in Lemma 3.8.

Proof. The first inequality follows easily from the definition of δ and by noting that the function $\frac{x}{\sqrt{1+x^2}} \leq \min(x, 1)$. For the second inequality, by the definition of δ we have that

$$\delta_2(\nu_1, x) - \delta_0(\nu_2, x) = \frac{\nu_1 - \nu_2}{x} + \frac{1}{2x} \left(\frac{\nu_1 + 1/2}{\sqrt{(\nu_1 + 1/2)^2 + x^2}} - \frac{\nu_2 - 1/2}{\sqrt{(\nu_2 - 1/2)^2 + x^2}} \right).$$

Now, consider the scalar function $f(x) = \frac{x}{\sqrt{1+x^2}}$ for $x \geq 0$. Note that the function is monotonically increasing, concave and has values between $[0, 1]$ with $f'(x) \leq f'(0) = 1$. Putting these facts together we have that for any $x_1 \geq x_2$

$$\frac{x_1}{\sqrt{1+x_1^2}} - \frac{x_2}{\sqrt{1+x_2^2}} \leq \min(x_1 - x_2, 1).$$

□

Using Lemma 3.8 and Lemma A.1 we have the following Lemma

Lemma A.2. *Given two non-negative integers ν, Δ we have that*

$$\log\left(\frac{I_\nu}{I_{\nu+\Delta}}\right) \leq \sum_{j=\nu+1}^{j=\nu+\Delta} \operatorname{arcsinh}(\delta_2(j, x)) \leq \min\left(\frac{\Delta^2 + 2\nu\Delta}{2x} \left(1 + \frac{1}{2x}\right) + \frac{\Delta}{2x^2}, \frac{\Delta^2 + 2\nu\Delta}{2x} + \frac{\Delta}{2x}\right)$$

$$\log\left(\frac{I_\nu(x)}{I_{\nu+\Delta}(x)}\right) \geq \sum_{j=\nu+1}^{j=\nu+\Delta} \operatorname{arcsinh}(\delta_0(j, x))$$

We are now ready to provide the proof of Lemma 3.7.

Proof of Lemma 3.7. We prove the statement for $\Delta \geq 0$, a similar analysis applies for the case $\Delta \leq 0$ by switching X to $-X$.

Since 3.8 applies only in the case when ν is positive, we need to handle the negative case via noting that for integer ν $I_\nu(x) = I_{|\nu|}(x)$. This necessitates the requirement for multiple cases. We begin with the first case

Case 1 - $X \geq \alpha\Delta$

In this case replacing setting $Y = X - \alpha\Delta$ we get that

$$\Phi_{X, \alpha, \Delta}(\mu) = \log\left(\frac{I_{Y+(\alpha-1)\Delta}(\mu)}{I_Y(\mu)} \left(\frac{I_{Y+(\alpha-1)\Delta}(\mu)}{I_{Y+\alpha\Delta}(\mu)}\right)^{\alpha-1}\right), \quad (\text{A.1})$$

where we know that $Y \geq 0$. Now consider the following calculation.

$$\begin{aligned}
\Phi_{X,\alpha,\Delta}(\mu) &\triangleq (\alpha - 1) \left(\sum_{i=Y+(\alpha-1)\Delta+1}^{Y+\alpha\Delta} \log \left(\frac{I_{i-1}(\mu)}{I_i(\mu)} \right) \right) - \sum_{i=Y+1}^{Y+(\alpha-1)\Delta} \log \left(\frac{I_{i-1}(\mu)}{I_i(\mu)} \right) \\
&= \sum_{j=0}^{\alpha-2} \left(\sum_{i=Y+(\alpha-1)\Delta+1}^{Y+\alpha\Delta} \log \left(\frac{I_{i-1}(\mu)}{I_i(\mu)} \right) - \sum_{i=Y+j\Delta+1}^{Y+j\Delta+\Delta} \log \left(\frac{I_{i-1}(\mu)}{I_i(\mu)} \right) \right) \\
&= \sum_{j=0}^{\alpha-2} \left(\sum_{i=Y+j\Delta+1}^{Y+j\Delta+\Delta} \left(\log \left(\frac{I_{i-1+(\alpha-1-j)\Delta}(\mu)}{I_{i+(\alpha-1-j)\Delta}(\mu)} \right) - \log \left(\frac{I_{i-1}(\mu)}{I_i(\mu)} \right) \right) \right) \\
&\leq \sum_{j=0}^{\alpha-2} \left(\sum_{i=Y+j\Delta+1}^{Y+j\Delta+\Delta} (\operatorname{arcsinh}(\delta_2(i + (\alpha - 1 - j)\Delta, \mu)) - \operatorname{arcsinh}(\delta_0(i, \mu))) \right) \\
&\leq \sum_{j=0}^{\alpha-2} \left(\sum_{i=Y+j\Delta+1}^{Y+j\Delta+\Delta} (\delta_2(i + (\alpha - 1 - j)\Delta, \mu) - \delta_0(i, \mu)) \right) \\
&\leq \sum_{j=0}^{\alpha-2} \left(\frac{(\alpha - 1 - j)\Delta^2}{\mu} + \min \left(\frac{(\alpha - 1 - j)\Delta^2 + \Delta}{2\mu^2}, \frac{\Delta}{2\mu} \right) \right) \\
&= \frac{\alpha(\alpha - 1)\Delta^2}{2\mu} + \min \left(\frac{\alpha(\alpha - 1)\Delta^2 + 2(\alpha - 1)\Delta}{4\mu^2}, \frac{(\alpha - 1)\Delta}{2\mu} \right),
\end{aligned}$$

where the first inequality follows from Lemma 3.8 and the second inequality follows from the fact that for all $0 \leq x \leq y$ we have that $\operatorname{arcsinh}(y) - \operatorname{arcsinh}(x) \leq y - x$ and the third inequality follows from Lemma A.1.

Case 2 - $X \leq 0$

In this case replacing setting $Y = -X$ we get that

$$\Phi_{X,\alpha,\Delta}(\mu) = \log \left(\frac{I_{Y+\Delta}(\mu)}{I_{Y+\alpha\Delta}(\mu)} \left(\frac{I_{Y+\Delta}(\mu)}{I_Y(\mu)} \right)^{\alpha-1} \right) \tag{A.2}$$

where we know that $Y \geq 0$. Now consider the following calculation.

$$\begin{aligned}
\Phi_{X,\alpha,\Delta}(\mu) &= \sum_{i=Y+\Delta+1}^{Y+\alpha\Delta} \log \left(\frac{I_{i-1}(\mu)}{I_i(\mu)} \right) - (\alpha - 1) \left(\sum_{i=Y+1}^{Y+\Delta} \log \left(\frac{I_{i-1}(\mu)}{I_i(\mu)} \right) \right) \\
&= \sum_{j=1}^{\alpha-1} \left(\sum_{i=Y+j\Delta+1}^{Y+j\Delta+\Delta} \log \left(\frac{I_{i-1}(\mu)}{I_i(\mu)} \right) - \sum_{i=Y+1}^{Y+\Delta} \log \left(\frac{I_{i-1}(\mu)}{I_i(\mu)} \right) \right) \\
&= \sum_{j=1}^{\alpha-1} \left(\sum_{i=Y+1}^{Y+\Delta} \left(\log \left(\frac{I_{i-1+j\Delta}(\mu)}{I_{i+j\Delta}(\mu)} \right) - \log \left(\frac{I_{i-1}(\mu)}{I_i(\mu)} \right) \right) \right) \\
&\leq \sum_{j=1}^{\alpha-1} \left(\sum_{i=Y+1}^{Y+\Delta} (\operatorname{arcsinh}(\delta_2(i + j\Delta, \mu)) - \operatorname{arcsinh}(\delta_0(i, \mu))) \right) \\
&\leq \sum_{j=1}^{\alpha-1} \left(\sum_{i=Y+1}^{Y+\Delta} (\delta_2(i + j\Delta, \mu) - \delta_0(i, \mu)) \right) \\
&\leq \sum_{j=1}^{\alpha-1} \left(\frac{j\Delta^2}{\mu} + \min \left(\frac{j\Delta^2 + \Delta}{2\mu^2}, \frac{\Delta}{2\mu} \right) \right)
\end{aligned}$$

$$= \frac{\alpha(\alpha-1)\Delta^2}{2\mu} + \min\left(\frac{\alpha(\alpha-1)\Delta^2 + 2(\alpha-1)\Delta}{4\mu^2}, \frac{(\alpha-1)\Delta}{2\mu}\right),$$

where the first inequality follows from Lemma 3.8 and the second inequality follows from the fact that for all $0 \leq x \leq y$ we have that $\operatorname{arcsinh}(y) - \operatorname{arcsinh}(x) \leq y - x$ and the third inequality follows from Lemma A.1.

Case 3 - $X \in [0, \Delta/2]$

In this case we first note that

$$\begin{aligned}\Phi_{X,\alpha,\Delta}(\mu) &= \log\left(\frac{I_{X-\Delta}(\mu)}{I_{X-\alpha\Delta}(\mu)} \left(\frac{I_{X-\Delta}(\mu)}{I_X(\mu)}\right)^{\alpha-1}\right) \\ &= \log\left(\frac{I_{\Delta-X}(\mu)}{I_{\alpha\Delta-X}(\mu)} \left(\frac{I_{\Delta-X}(\mu)}{I_X(\mu)}\right)^{\alpha-1}\right)\end{aligned}$$

Next consider the following calculation which corresponds to applying Lemma A.2 to the above expression we get that,

$$\Phi_{X,\alpha,\Delta}(\mu) \leq \sum_{j=\Delta-X+1}^{\alpha\Delta-X} \operatorname{arcsinh}(\delta_2(j, \mu)) - (\alpha-1) * \left(\sum_{j=X+1}^{\Delta-X} \operatorname{arcsinh}(\delta_0(j, \mu))\right)$$

We again intend to use the inequality $\operatorname{arcsinh}(y) - \operatorname{arcsinh}(x) \leq y - x$ for $y \geq x$. To this end first note that the number of terms on the left summation in the above inequality are at least as many as the number of terms on the RHS (taking the multiplicity via $\alpha-1$ into account). Therefore for those terms we can apply the above inequality. For the remaining we simply use the inequality $\operatorname{arcsinh}(x) \leq x$. Therefore we get the following simplification,

$$\Phi_{X,\alpha,\Delta}(\mu) \leq \sum_{j=\Delta-X+1}^{\alpha\Delta-X} \delta_2(j, \mu) - (\alpha-1) * \left(\sum_{j=X+1}^{\Delta-X} \delta_0(j, \mu)\right).$$

We can now use the upper and lower bounds on δ_2, δ_0 given by Lemma A.1. To this end consider the following calculation,

$$\begin{aligned}&\sum_{j=\Delta-X+1}^{\alpha\Delta-X} \frac{j-1/2}{\mu} - (\alpha-1) * \left(\sum_{j=X+1}^{\Delta-X} \frac{j-1/2}{\mu}\right) \\ &= \frac{(\alpha-1)^2\Delta^2 + 2(\Delta-X)(\alpha-1)\Delta}{2} - (\alpha-1) \left(\frac{(\Delta-2X)^2 + 2X(\Delta-2X)}{2}\right) \\ &= \frac{\alpha(\alpha-1)\Delta^2}{2\mu}.\end{aligned}$$

Now a direct application of Lemma A.1 yields

$$\log\left(\frac{I_{\Delta-X}(\mu)}{I_{\alpha\Delta-X}(\mu)} \left(\frac{I_{\Delta-X}(\mu)}{I_X(\mu)}\right)^{\alpha-1}\right) \leq \frac{\alpha(\alpha-1)\Delta^2}{2\mu} + \min\left(\frac{(\alpha+1)(\alpha-1)\Delta^2}{4\mu^2} + \frac{(\alpha-1)\Delta}{2\mu^2}, \frac{(\alpha-1)\Delta}{2\mu}\right).$$

Case 4 - $X \in [\Delta/2, \Delta]$

In this case we first note that

$$\Phi_{X,\alpha,\Delta}(\mu) = \log\left(\frac{I_{X-\Delta}(\mu)}{I_{X-\alpha\Delta}(\mu)} \left(\frac{I_{X-\Delta}(\mu)}{I_X(\mu)}\right)^{\alpha-1}\right)$$

$$= \log \left(\frac{I_{\Delta-X}(\mu)}{I_{\alpha\Delta-X}(\mu)} \left(\frac{I_{\Delta-X}(\mu)}{I_X(\mu)} \right)^{\alpha-1} \right)$$

Next consider the following calculation which corresponds to applying Lemma A.2 to the above expression and collecting the terms corresponding to $\frac{\Delta^2+2\nu\Delta}{2x}$ in the lemma in this context.

$$\frac{(\alpha-1)^2\Delta^2 + 2(\Delta-X)(\alpha-1)\Delta}{2} + \frac{(2X-\Delta)^2 + 2(\Delta-X)(2X-\Delta)}{2} = \frac{\alpha(\alpha-1)\Delta^2}{2\mu}$$

Now a direct application of Lemma A.2 yields

$$\log \left(\frac{I_{\Delta-X}(\mu)}{I_{\alpha\Delta-X}(\mu)} \left(\frac{I_{\Delta-X}(\mu)}{I_X(\mu)} \right)^{\alpha-1} \right) \leq \frac{\alpha(\alpha-1)\Delta^2}{2\mu} + \min \left(\frac{\alpha(\alpha-1)\Delta^2}{4\mu^2} + \frac{3(\alpha-1)\Delta}{2\mu^2}, \frac{3(\alpha-1)\Delta}{2\mu} \right).$$

Case 5 - $X \in [\Delta, (\alpha+1)\Delta/2]$

In this case we first note that

$$\begin{aligned} \Phi_{X,\alpha,\Delta}(\mu) &= \log \left(\frac{I_{X-\Delta}(\mu)}{I_{X-\alpha\Delta}(\mu)} \left(\frac{I_{X-\Delta}(\mu)}{I_X(\mu)} \right)^{\alpha-1} \right) \\ &= \log \left(\frac{I_{X-\Delta}(\mu)}{I_{\alpha\Delta-X}(\mu)} \left(\frac{I_{X-\Delta}(\mu)}{I_X(\mu)} \right)^{\alpha-1} \right) \end{aligned}$$

Next consider the following calculation which corresponds to applying Lemma A.2 to the above expression and collecting the terms corresponding to $\frac{\Delta^2+2\nu\Delta}{2x}$ in the lemma in this context.

$$\frac{(\alpha-1)(\Delta^2 + 2(X-\Delta)\Delta)}{2} + \frac{((\alpha+1)\Delta - 2X)^2 + 2(X-\Delta)((\alpha+1)\Delta - 2X)}{2} = \frac{\alpha(\alpha-1)\Delta^2}{2\mu}$$

Now a direct application of Lemma A.2 yields

$$\log \left(\frac{I_{X-\Delta}(\mu)}{I_{\alpha\Delta-X}(\mu)} \left(\frac{I_{X-\Delta}(\mu)}{I_X(\mu)} \right)^{\alpha-1} \right) \leq \frac{\alpha(\alpha-1)\Delta^2}{2\mu} + \min \left(\frac{\alpha(\alpha-1)\Delta^2}{4\mu^2} + \frac{(\alpha-1)\Delta}{2\mu^2}, \frac{(\alpha-1)\Delta}{2\mu} \right).$$

Case 6 - $X \in [(\alpha+1)\Delta/2, \alpha\Delta]$

In this case we first note that

$$\begin{aligned} \Phi_{X,\alpha,\Delta}(\mu) &= \log \left(\frac{I_{X-\Delta}(\mu)}{I_{X-\alpha\Delta}(\mu)} \left(\frac{I_{X-\Delta}(\mu)}{I_X(\mu)} \right)^{\alpha-1} \right) \\ &= \log \left(\frac{I_{X-\Delta}(\mu)}{I_{\alpha\Delta-X}(\mu)} \left(\frac{I_{X-\Delta}(\mu)}{I_X(\mu)} \right)^{\alpha-1} \right) \end{aligned}$$

Next consider the following calculation which corresponds to applying Lemma A.2 to the above expression we get that,

$$\Phi_{X,\alpha,\Delta}(\mu) \leq (\alpha-1) * \left(\sum_{j=X-\Delta+1}^X \operatorname{arcsinh}(\delta_2(j, \mu)) \right) - \sum_{j=\alpha\Delta-X+1}^{X-\Delta} \operatorname{arcsinh}(\delta_0(j, \mu))$$

We again intend to use the inequality $\operatorname{arcsinh}(y) - \operatorname{arcsinh}(x) \leq y - x$ for $y \geq x$. To this end first note that the number of terms on the left summation in the above inequality are at least as many as the number of terms on the RHS (taking the multiplicity via $\alpha-1$ into account). Therefore for those terms we can apply

the above inequality. For the remaining we simply use the inequality $\operatorname{arcsinh}(x) \leq x$. Therefore we get the following simplification,

$$\Phi_{X,\alpha,\Delta}(\mu) \leq (\alpha - 1) * \left(\sum_{j=X-\Delta+1}^X \delta_2(j, \mu) \right) - \sum_{j=\alpha\Delta-X+1}^{X-\Delta} \delta_0(j, \mu).$$

We can now use the upper and lower bounds on δ_2, δ_0 given by Lemma A.1. To this end consider the following calculation,

$$\begin{aligned} & (\alpha - 1) * \left(\sum_{j=X-\Delta+1}^X \frac{j - 1/2}{\mu} \right) - \sum_{j=\alpha\Delta-X+1}^{X-\Delta} \frac{j - 1/2}{\mu} \\ &= \frac{(\alpha - 1)(\Delta^2 + 2(X - \Delta)\Delta)}{2} - \frac{(2X - (\alpha + 1)\Delta)^2 + 2(\alpha\Delta - X)((2X - (\alpha + 1)\Delta))}{2} \\ &= \frac{\alpha(\alpha - 1)\Delta^2}{2\mu}. \end{aligned}$$

Now a direct application of Lemma A.2 yields

$$\log \left(\frac{I_{X-\Delta}(\mu)}{I_{\alpha\Delta-X}(\mu)} \left(\frac{I_{X-\Delta}(\mu)}{I_X(\mu)} \right)^{\alpha-1} \right) \leq \frac{\alpha(\alpha - 1)\Delta^2}{2\mu} + \min \left(\frac{(2\alpha - 1)(\alpha - 1)\Delta^2}{4\mu^2} + \frac{(\alpha - 1)\Delta}{\mu^2}, \frac{(\alpha - 1)\Delta}{\mu} \right).$$

□

B Additional Results

B.1 Shakespeare

We additionally evaluate our methods on Shakespeare, a public federated language modeling dataset [31, 41]. The dataset is built on the collective works of William Shakespeare, where each of the total $N = 715$ clients corresponds to a speaking role with at least two lines. The task of this dataset is to predict the next word based on the preceding words in a line. The dataset is split into training set and test set by partitioning the lines from each client. The model used for this task follows that of [41], to which we refer the reader for more details on the dataset and the experimental setup.

Our hyperparameters mostly follow those from [6, 41] and limited tuning was performed; see Table 2 for a complete list of hyperparameters. We do a small grid search over the ℓ_2 clipping values $c \in \{0.25, 0.5\}$. We set the number of clients per round $n = 100$ and we train for $T = 1200$ rounds. In particular, note that it is challenging to obtain a small ε on this dataset due to the small N and the minimal n sufficient for convergence; we thus follow [6] and [33] to report privacy with a hypothetical population size $N = 10^6$.

Figure 6 compares the test accuracies (averaged over the last 100 rounds) across different mechanisms and values of ε and b . Figure 7 compares the mechanisms during training. The optimal clipping is $c = 0.5$ for $\varepsilon = 7.5$ and $c = 0.25$ otherwise. Note that Skellam matches DDGauss across all settings. The slight performance gap from both Skellam and DDGauss to Gaussian is likely due to the effects of modular clipping error from SecAgg (cf. Figure 10).

B.2 Federated EMNIST

Figure 8 includes the omitted details of Figure 5 (left) and illustrates the effect of a larger k . Figure 9 compares the test accuracies of different methods on EMNIST over training $T = 1500$ rounds for different values of ε and b with $k = 3$.

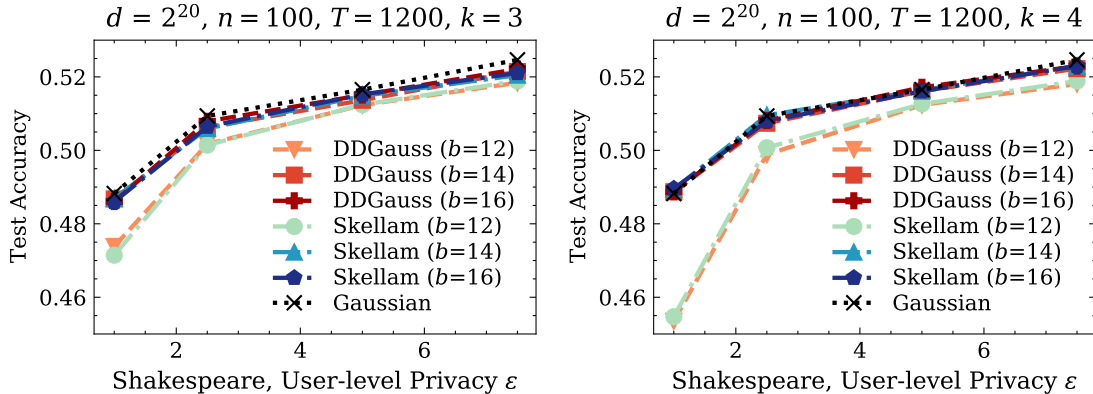


Figure 6: Summary of test accuracies on **Shakespeare** across different ϵ and b averaged over the last 100 rounds with a hypothetical population size $N = 10^6$. $\delta = 10^{-6}$. **Left:** $k = 3$. **Right:** $k = 4$.

B.3 Stack Overflow Next Word Prediction

Figure 10 illustrates the effect of k on the test accuracies. Note that for $k = 3$, there is a slight performance gap between Gaussian and Skellam/DDGauss likely due to the modular clipping error introduced by SecAgg. By increasing k , we can reduce scaling and sacrifice quantization errors to close the gap. Figure 11 additionally shows the accuracies on the validation set over training $T = 1600$ rounds for different values of ϵ and b with $k = 4$.

B.4 Comparison against Discrete Laplace

Figure 12 compares Skellam and (discrete) Gaussian against the discrete Laplace mechanism under various accounting schemes on privacy compositions.

C Additional Details

C.1 Models for FL experiments

For Federated EMNIST, we use a small convolutional network similar to the architecture used in [41]. Our architecture is slightly smaller and has $\bar{d} < 2^{20}$ parameters to reduce the zero padding required by the randomized Hadamard transform (see Algorithm 1). The architecture is summarized in Table 1. For Stack Overflow NWP and Shakespeare (Section B.1), we use the architectures from [41] directly.⁵

C.2 Datasets

License, Availability, and Curation The federated datasets used in our FL experiments (Federated EMNIST [14], Stack Overflow Next Word Prediction [8], and Shakespeare [31]) are publicly available⁶ from TensorFlow Federated [24]. To our knowledge, they have been appropriately anonymized and do not contain personally identifiable information. Federated EMNIST and Shakespeare is licensed under the BSD 2-Clause License, while SO-NWP uses the CC BY-SA 3.0 License.

Dataset Splits For all FL datasets, we used the standard dataset split provided by TensorFlow. For EMNIST and Shakespeare, the datasets are split into training set and test set, and performance is reported on the test set. For Stack Overflow NWP, the dataset is split into training, validation, and test sets; the

⁵<https://github.com/google-research/federated/tree/master/utils/models>

⁶https://www.tensorflow.org/federated/api_docs/python/tff/simulation/datasets

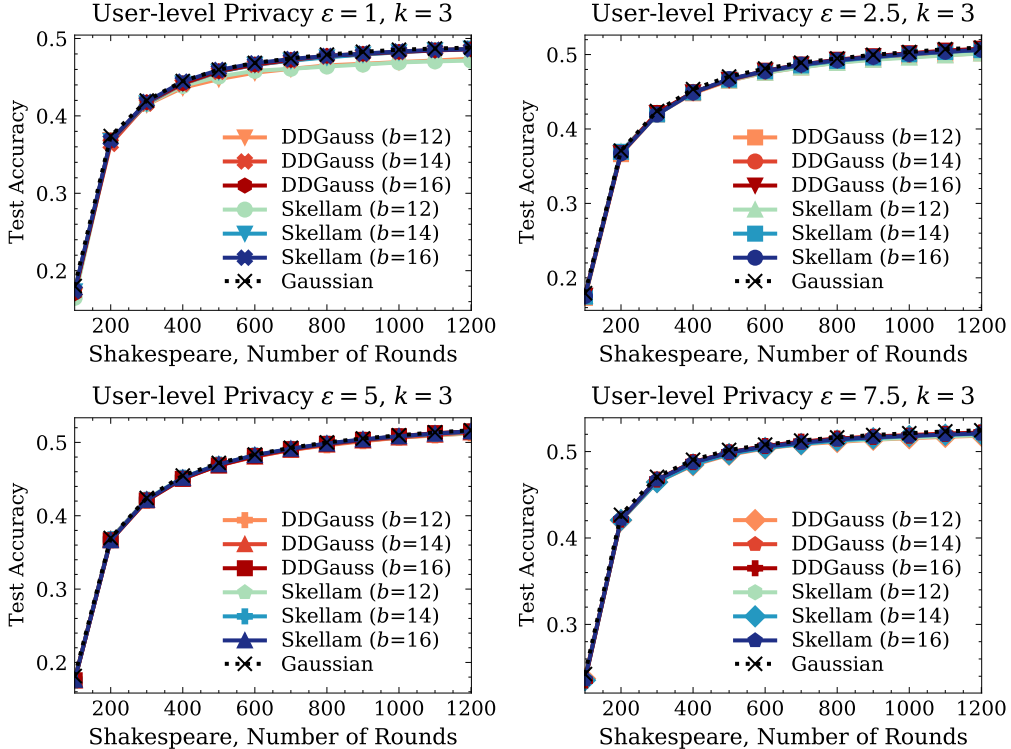


Figure 7: Test accuracies on **Shakespeare** over training $T = 1200$ rounds (averaged every 100 rounds) with a hypothetical population size $N = 10^6$. $\delta = 10^{-6}$. $k = 3$.

summary plots (e.g. Figure 10) report performance on the test set and the validation plots (e.g. Figure 11) report performance on the validation set. While other validation metrics/methods are possible, we note that using the dataset splits available from TensorFlow is standard practice in recent work (e.g. [41, 25, 33, 3]) and it allows our methods to be comparable in similar settings. Note also that validation data are often unavailable for training real-world FL models, and techniques such as k -fold validation can incur additional privacy costs.

C.3 Other Implementation Details

Privacy Amplification via Sub-sampling The privacy guarantees for FL experiments leverage amplification via sub-sampling as a subset of the clients is selected in each of the T rounds to participate in training (we use [37] for Gaussian and [51] for Skellam and DDGauss). We note that the underlying assumptions – that the clients can be sampled uniformly, and that the identities of the clients can be hidden from the sampler – do not always hold, particularly in federated learning settings where the availability of the clients can be different at each round and the central server is the entity initiating the training/sampling procedure. However, we note that the privacy guarantees is applicable for external analysts that request the trained model from the central aggregator.

Random seeds For all experiments, we fixed both the seed for the client dataset randomness (sampling, shuffling, etc.) and the seed of initializing the parameters of the model architectures. Note that the FL experiments are not repeated for multiple seeds due to computational costs, though the test accuracies on EMNIST/Shakespeare and the validation accuracies on SO-NWP are averaged over the last 100 rounds.

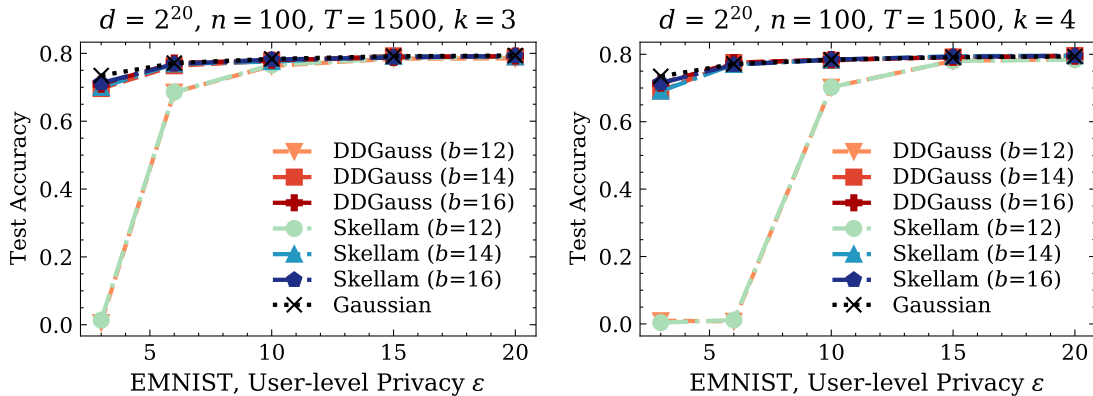


Figure 8: Summary of test accuracies on **Federated EMNIST** across different ϵ and b averaged over the last 100 rounds. $\delta = 1/N$. **Left:** $k = 3$. **Right:** $k = 4$.

Layer	Output Shape	# Params
Input	$28 \times 28 \times 1$	0
Conv 3×3 , 32	$26 \times 26 \times 32$	320
MaxPool	$13 \times 13 \times 32$	0
Conv 3×3 , 64	$11 \times 11 \times 64$	18496
Dropout, 25%	$11 \times 11 \times 64$	0
Flatten	7744	0
Dense	128	991360
Dropout, 25%	128	0
Dense	62	7998
Total # Params		1018174

Table 1: Model architecture for Federated EMNIST.

Hyperparameters Table 2 summarizes the hyperparameters used for the FL experiments. We adopt most hyperparameters from previous work and tuning is limited. We follow [25] for EMNIST, [6] for Shakespeare, and [27] for Stack Overflow NWP. We sweep different server learning rates for SO-NWP and different clipping thresholds c for Shakespeare and report the best results. We also show the effect of k on the trade-off between modular clipping error and quantization error (e.g. Figure 10), though the same values of k is used when comparing different methods.

D Practical Remarks

D.1 Ease of Sampling

One of the practical advantages of the Skellam mechanism compared to the (distributed) discrete Gaussian mechanism is that the sampling routines for Skellam (Poisson) distribution are widely available in data analysis and machine learning software packages such as NumPy, TensorFlow, and PyTorch that ML / DP practitioners would use for development. However, we’d like to point out that discrete Gaussian sampling itself has been well explored in the lattice-based cryptography community (e.g., [43, 18, 38]) and we would expect that the efficient sampling routines (often implemented in C/C++, e.g. [4]) would perform as good as optimized Poisson samplers if compared under a similar setting. While it is perceivable that discrete Gaussian samplers will become more accessible for ML and DP practitioners in the future, the discrete Gaussian has only recently been introduced [15] in the differential privacy context and thus the Skellam

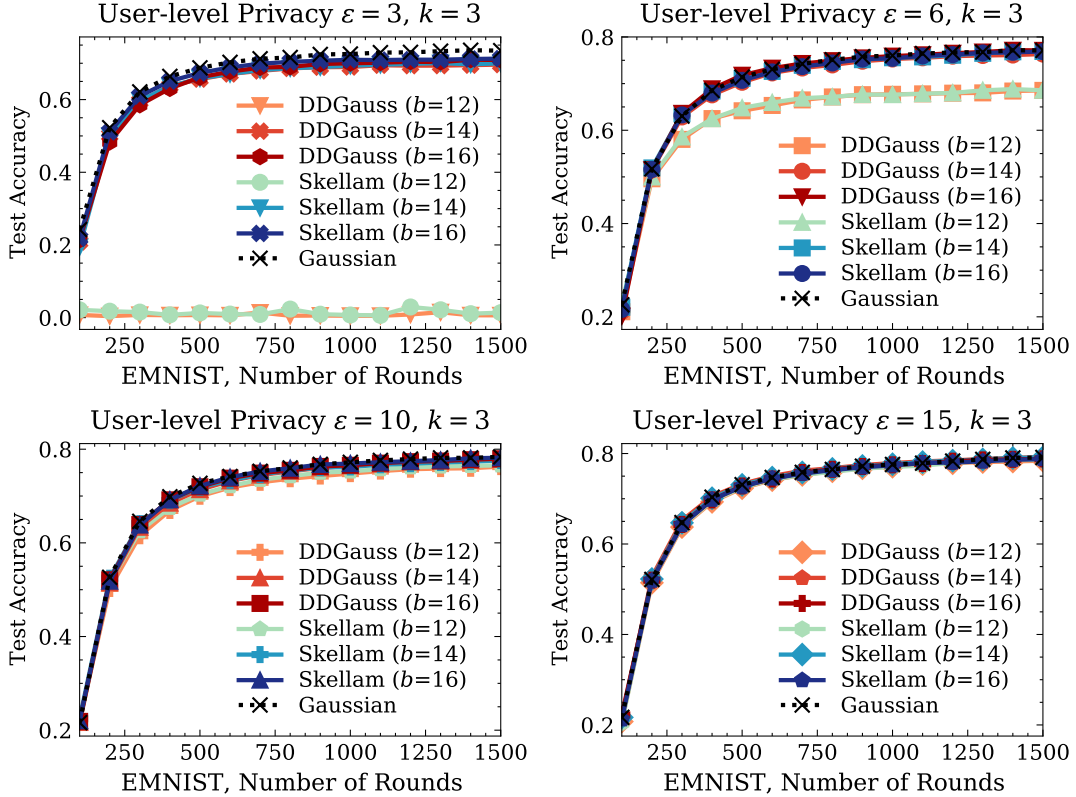


Figure 9: Test accuracies on **Federated EMNIST** over training $T = 1500$ rounds (averaged every 100 rounds). $\delta = 1/N$. $k = 3$.

mechanism provides a practical advantage as differentially private FL systems with compression and scalable secure aggregation are near deployment today. We also provide a preliminary comparison of the sampling time against two existing implementations of discrete Gaussian sampler [15, 25] available to DP practitioners; the implementation from [15] is not vectorized and thus can be $1000\times$ slower than Skellam sampling, and the implementation from [25] is still up to 40% slower in TensorFlow eager execution.

D.2 Closure Under Summation

The property that Skellam samples are closed under summation gives several practical advantages.

From a theoretical standpoint, being closed under summation removes the need for accounting for the divergence errors, which, as measured in DDGauss [25] as an infinity divergence, grow with the number of clients (as opposed to no such dependence for Skellam), which can be problematic with settings of massively distributed client base (e.g. federated analytics).

Concretely, consider the simple quantile estimation problem [6] where we have a large number of clients ($n \geq 1000$) and sensitivity-1 (binary) queries. With a large central noise standard deviation $\sigma_c \geq 5$, we can achieve a strong privacy (as $\epsilon \approx \Delta/\sigma_c$), but if this noise is to be added locally (via the distributed DP with SecAgg model), the τ term of DDGauss (Thm 1 of [25]) would significantly degrade the privacy guarantees because large n means more additive divergence terms and smaller local noise standard deviation which (exponentially) widens the divergence – this effect can be inferred from the left of Figure 2 where DDGauss underperforms at small noise levels and, in comparison, Skellam degrades more gracefully with smaller noises. For a specific example, consider $n = 10000$ and $\sigma_c = 50$; in this case, the local noise standard deviation $\sigma_l = 0.5$, and at $\alpha = 2$, the RDP $\epsilon(\alpha)$ of Gaussian and Skellam is 4×10^{-4} and 4.0036×10^{-4}

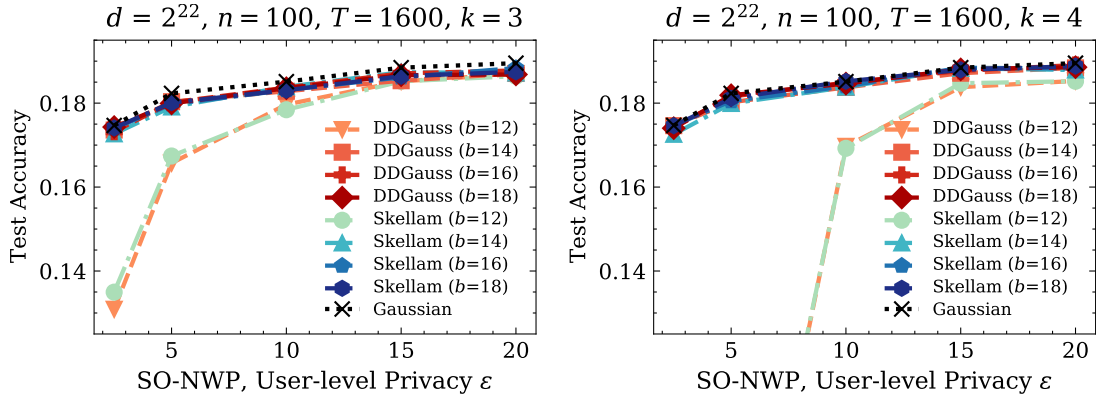


Figure 10: Summary of test accuracies on **Stack Overflow NWP** across different ϵ and b . $\delta = 10^{-6}$. **Left:** $k = 3$. **Right:** $k = 4$.

	EMNIST	Shakespeare	Stack Overflow NWP
Client LR η_{client}	0.32	1	0.5
Server LR η_{server}	1	0.32	{0.3, 1}
Server momentum	0.9	0.9	0.9
Client Batch Size	20	4	16
Client epochs per round	1	1	1
Max examples per client	-	-	256
Clients uniform weighting	✓	✓	✓
ℓ_2 clipping c	0.03	{0.25, 0.5}	0.3
Clients per round n	100	100	100
Population size N	3400	715 [‡]	342477
Training rounds T	1500	1200	1600
Conditional rounding bias [†] β	$\exp(-0.5)$	$\exp(-0.5)$	$\exp(-0.5)$
Privacy δ	$1/N$	10^{-6}	10^{-6}

Table 2: Summary of hyperparameters for the FL experiments. [†]Discrete mechanisms only. [‡]A hypothetical population size $N = 10^6$ was used when reporting privacy guarantees.

respectively, while the RDP of DDGauss is > 723 (a factor of $> 10^6$) due to the sum divergence term τ . While scaling both the raw values and the noise variances can help alleviate this issue, it also introduces additional communication costs.

From an engineering perspective, while the divergence term for discrete Gaussian is usually small enough, we still need to keep track of it and its dependent parameters (number of clients, client dimensions, variance) for privacy accounting. Skellam on the other hand only requires us to track the variance and thereby allows easier switching between central DP (noise on the server) and distributed DP (noise on the clients) implementations.

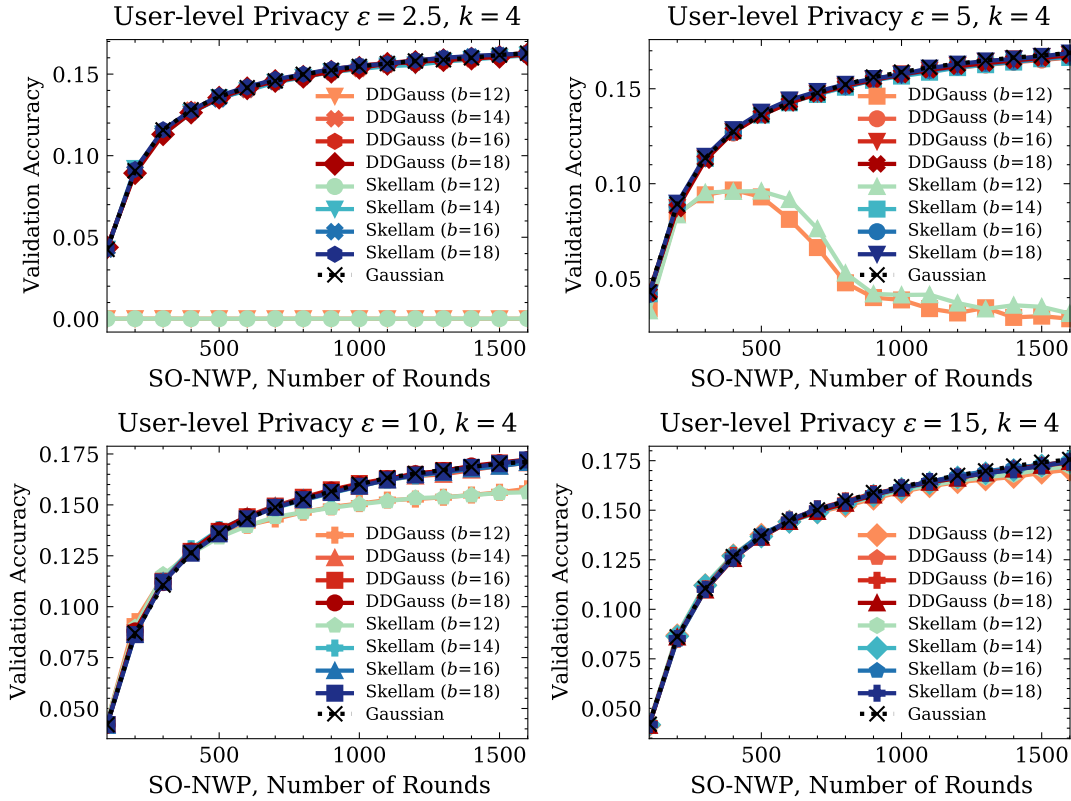


Figure 11: Validation accuracies on **Stack Overflow NWP** over training $T = 1600$ rounds (averaged every 100 rounds). $\delta = 10^{-6}$. $k = 4$.

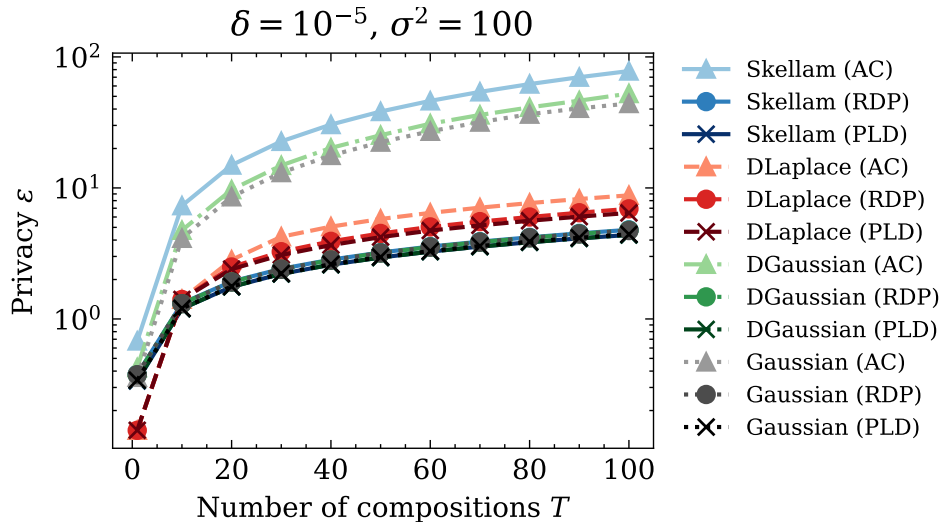


Figure 12: Comparing privacy compositions across various mechanisms in the scalar case. $\Delta = 1$. DLaplace: Discrete Laplace. DGaussian: Discrete Gaussian. AC: Advanced Composition. RDP: Rényi DP. PLD: Privacy Loss Distributions.